Journal of the Brazilian Society of Mechanical Sciences and Engineering (2018) 40:310
https://doi.org/10.1007/s40430-018-1235-0

TECHNICAL PAPER

Parametric study on the dry sliding wear behaviour of AA6082–T6/TiB_2 in situ composites using response surface methodology

Gurpreet Singh[1] · Sammy Lap-Ip Chan[2] · Neeraj Sharma[3]

Received: 23 August 2017 / Accepted: 15 May 2018 / Published online: 26 May 2018

Abstract

Present work deals with the parametric study of dry sliding wear behaviour of TiB_2-reinforced aluminium matrix composites (AMCs). Aluminium 6082-T6 alloy specimens reinforced with 0, 3, 6, 9 and 12 wt% of TiB_2 particles were fabricated by the in situ reaction of K_2TiF_6 and KBF_4 in heated liquid aluminium. Experiments were conducted to study the wear behaviour of AA6082–T6/TiB_2 composites using pin-on-disc apparatus at room temperature. Weight percentage of reinforcement, sliding speed, load and sliding distance were the process parameters studied in the present investigation, with five different levels of each parameter. The parametric optimization was done employing response surface methodology. The results confirmed that an increase in the amount of reinforcement and sliding speed decreased the wear loss, and an increase in load and sliding distance increased the wear in TiB_2-reinforced AMCs. However, the relative significance of these parameters on the sliding wear resistance of the AMCs was very much different. Analysis of variance showed that the sliding distance was the most dominating factor with 65.28% to influence the wear loss in the fabricated composites; it was preceded by the sliding speed with 14.78%, load (9.39%) and reinforcement percentage (3.86%), respectively. The present model was validated by conducting confirmation tests. Thus in this work an accurate wear model has been developed, and it can be used as a predictive tool for wear applications.

Keywords AA6082–T6/TiB_2 composites · Sliding wear · Response surface methodology · Predictive tool

1 Introduction

Aluminium-based metal matrix composites (AMCs) have been the topic of research for a number of years, owning to the remarkable properties they exhibit such as high thermal conductivity and high specific strength [1]. These properties make them an attractive material in the various aerospace and automotive applications. Hard particles, such as SiC, B_4C, Al_2O_3, TiC, Si_3N_4, TiB_2, have been used as reinforcements for AMCs, so as to improve the mechanical properties of the composites. However, at the same time the hardness of these ceramic additives also contributes to the wear of the material. The hard particles can easily penetrate through the metal during the sliding operations and uproot the material in the form of small lumps [2]. This aspect influences the overall performance of not only the composites but of all the tribological pairs.

Among all the ceramic particles, TiB_2 emerged as an eminent material, attributable to its high stiffness and hardness, and more importantly TiB_2 and aluminium do not produce any detrimental by-product at the interface between the molten Al matrix and the reinforcement [3]. TiB_2 is also a preferable reinforcement for AMCs when the wear resistance is an important consideration [4]. The strong bonding between TiB_2 and aluminium alloy increases the hardness of the AMCs and enhances the wear resistance of the fabricated composite. Al–TiB_2 composites find applications in the high-tech structural and the operational areas including defence, automotive, aerospace and in the field of sports [5].

As reported in the literature, several aspects regarding TiB_2-reinforced composites have been studied. Mandal

Technical Editor: Paulo de Tarso Rocha de Mendonça.

✉ Gurpreet Singh
gurpreet.er85@gmail.com

[1] AIT, Amity University, Noida, U.P. 201313, India

[2] School of Materials Science and Engineering, University of New South Wales, Sydney, NSW 2033, Australia

[3] Department of Mechanical Engineering, Maharishi Markandeshwar (Deemed to be University), Mullana, Ambala, Haryana 133207, India

et al. [6] investigated the wear behaviour of Al–4Cu–TiB_2 composites using different loads and reported that the addition of TiB_2 in aluminium alloy increased the wear resistance of the composites significantly. Kumar et al. [7] fabricated the TiB_2-reinforced composite through in situ process using Al–7Si alloy and observed that the wear resistance and the mechanical properties of the alloy with TiB_2 has increased as compared to the base alloy. Mandal et al. [8] fabricated A356–TiB_2 composites and reported that the wear rate was a strong function of TiB_2 content as the addition of TiB_2 improved the wear resistance properties of the composites appreciably. In a study by Mallikarjuna et al. [9], exothermic reaction between K_2TiF_6 and KBF_4 salts at 8500 °C was used to fabricate AA2014/TiB_2 composites, and the results showed that TiB_2 was effectual in enhancing the wear resistance and in reducing the friction coefficient of the AMCs. In another study conducted by Ramesh and Ahmed [10], dry sliding friction and wear behaviour of AA6063/TiB_2 composites were analysed using a load range of 10–15 N and sliding velocity ranged from 0.209 to 1.256 m/s. The results revealed low coefficient of friction and wear rates in the fabricated composites as compared to those of the base alloy under all test conditions. The analysis of Ramesh and Ahmed [10] also showed that the wear rate of both the monolithic alloy and the in situ composite increased with increase in both the load and sliding velocity, whereas the coefficient of friction decreased with increase in load and increased with increase in sliding velocity. Niranjan and Lakshminarayanan [11] investigated the wear behaviour of TiB_2-reinforced in situ aluminium composites under loadings of 40, 50, and 60 N, respectively; and observed a significant improvement in wear properties of the composites. Another study was conducted by Radhika and Raghu [12] where Al–$Si_{12}Cu$/TiB_2 metal matrix composites was fabricated by liquid metallurgy route; they used response surface methodology (RSM) to relate various sliding parameters with the dry sliding wear characteristics of the composites. The regression test showed that a higher order of velocity significantly affected the wear rate of the composites. There are also works on other reinforcements to study the mechanical characterization of AMC's by adopting different methodologies [13–17].

Given the vast amount of experimental works found in the literature, the parametric study on wear behaviour of Al6082–T6/TiB_2, however, is limited. To the knowledge of the present authors, no research till date uses RSM to study the wear properties of Al6082–T6/TiB_2 composites. In this work, AMCs were fabricated by the in situ reaction of K_2TiF_6 and KBF_4 in the heated liquid aluminium and the sliding wear behaviour of AA6082–T6/TiB_2 composites was evaluated. The present work aims to establish a RSM model on the influence of four parameters, namely reinforcement content, sliding speed, load and sliding distance, on the wear performance of these composites. As RSM is considered as an effective tool for process optimization, it has been used here for the planning of experiments and modelling of the four process parameters. Here, the authors took five levels of each parameter to study their influences on the wear behaviour of AA6082–T6/TiB_2 composites. Confirmation tests were employed to validate the predictive model developed in this work.

2 Experimental details

2.1 Materials and composite fabrication

The chemical composition of the starting material AA6082–T6 used in the present work is shown in Table 1. The base alloy was cut into small rectangular slabs and weighted for the fabrication of composites. One kilogram of commercially available AA6082–T6 was placed in a graphite crucible and melted at a temperature of 800 °C using an electric furnace. The quantities of the inorganic salts potassium hexaflurotitanate (K_2TiF_6) and potassium tetrafluroborate (KBF_4) added to the molten aluminium are given in Table 2. The mixture containing K_2TiF_6, KBF_4 and molten aluminium was stirred continuously for 20–25 min with a graphite stirrer at 400 rpm, to ensure uniform distribution of the salts within the melt. This was an essential step to facilitate the reaction between the salts for the in situ production of titanium diboride (TiB_2). As can be seen from Table 2, by varying the amounts of the salts added, AMC casts with 3–12 wt% of TiB_2 can be obtained. After removal of the slag, the liquid mixture was poured in a preheated die made of sand and allowed to cool down and solidify. Artificial ageing was done to improve the strength and hardness of the material. Each specimen was reheated to 200 °C for 6 h then allowed to cool in the open atmosphere.

2.2 Microstructure analysis

The cylindrical samples with 6 mm diameter and 30 mm height were prepared from the casts for microstructural and hardness studies. All specimens were ground with emery paper of grade 400, 600 and 1000 and polished with diamond paste using polishing machine. Keller's reagent containing 2 ml HF, 3 ml HCl, 20 ml HNO_3 and 175 ml H_2O was used to reveal the microstructure. Scanning electron microscope (JOEL JSM-6510LV) was used to study the microstructure of the composites.

XRD patterns were recorded using a PANalytical X'pert PRO X-ray diffractometer. The patterns were carried out on the diffractometer with CuK radiation $\lambda = 1.54$ Å. The

Table 1 Chemical composition of AA6082–T6

Element	Mg	Si	Mn	Fe	Cu	Cr	Zn	Ti	Vn	Al
Content (wt%)	0.69	0.91	0.56	0.23	0.06	0.035	0.098	0.019	0.01	97.4

Table 2 Amount of salts added to molten aluminium to obtain in situ TiB_2

TiB_2 (wt%)	0	3	6	9	12
K_2TiF_6 (g)	0	110	230	350	470
KBF_4 (g)	0	140	290	450	600

diffraction angle was taken from 20° to 110° during the analysis.

2.3 Microhardness evaluation

The microhardness tests were performed using a Vickers hardness tester (Mitutoyo make) following the test method IS 1501-2002, at a load of 1 kg applied for 15 s [18]. Each of the specimens was tested three times at different positions on the specimen, and the average value has been taken.

2.4 Wear tests

A pin-on-disc apparatus (Ducom make) was used to execute wear tests for the analysis of wear behaviour of AA6082–T6/TiB_2 composites. All the tests were performed at room temperature of 20–25 °C and a relative humidity of 25–30%. EN31 steel disc with a hardness of 860 HV and a surface roughness of 0.1 Ra (µm) was used as a countersurface. Figure 1 shows the schematic of the apparatus utilized in the present work. The specimen as the wear pin was clutched stationary adjacent to the counter surface and a lever mechanism was used to apply the normal load.

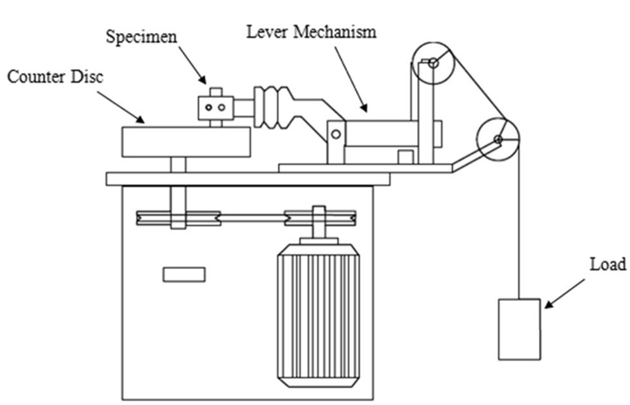

Fig. 1 Pin-on-disc apparatus used in the present work

Acetone was used to clean the pin and the countersurface before each run of experiment so as to make dirt-free and dry sliding conditions. The wear loss of the sample was weighted by a digital weight balance with an accuracy of 0.0001 g was used for this purpose.

2.5 Response surface methodology (RSM)

Microhardness and normal load significantly affect the material removal rate during sliding in a number of mechanical operations [19]. The microhardness also depends upon the type and the quantity of reinforcement added in the aluminium composites; and consequently weight percentage of reinforcement and load were selected as process parameters in the present work. Two additional factors, i.e., sliding speed and sliding distance, have also been included in the study. In order to optimize the process parameters, RSM was employed in which five different levels were selected for each process parameter. Researchers in the past also used the technique of RSM and studied the effect of different factors and the interactions among them on the analysis of the wear behaviour of materials as it is one of the effective tools for process optimization [20, 21].

The below-mentioned steps are followed to apply the RSM:

1. The first step in RSM is the development of trial experiments.
2. Input parameters are designed according to trial experiments or literature review and selection of response variables according to the requirement.
3. Selection of experimental design in line with the process parameters and their levels.
4. After the selection of experimental design, the regression analysis is to be performed.
5. Analysis of variance (ANOVA) is to be studied for the evaluation of the process parameters.
6. If the model is significant and lack of fit is non-significant, then optimal setting is to be found out.
7. At the suggested setting, validation experiments are performed
8. If model is not significant, then the screening of the input parameters is to be carried out and repeat the process from step 3.

The experiments were constructed employing central composite design (CCD) as it is considered to be an effectual tool for building a model when the number of factors is high [22]. Factors and the levels used in CCD experimental plan given in Table 3. According to Rabinowicz's classic theory [19], the applied load and hardness (which varies with addition of reinforcement) of materials are the most important factors affecting the wear process. Therefore, both these factors were considered along with the sliding speed and sliding distance in this study. Thus, four factors, i.e., % reinforcement: load, sliding speed, and sliding distance were used in the present study. The central composite design (CCD) used in the present study contains factorial points each at upper (+ 1) and lower (− 1) values, centre points (0) and axial points of upper (+ 2) and lower (− 2) values. In this way, five levels of each process parameter were chosen in CCD.

In the present work, the maximum % of reinforcement used for composite fabrication was 12 (as higher % of reinforcement may results in higher agglomeration of particles which in turn hamper the mechanical properties), so five levels were selected as 0, 3, 6, 9 and 12. The exact dead weight's of size 0.1,0.5,1 and 2 kg are provided with pin-on-disc to vary the load so in order to take five different levels of load, and the authors have selected the five levels as 1.5, 3, 4.5 and 6 kg, i.e., (14.71, 29.42, 44.13, 55.84 and 73.55 N). The levels of sliding speed were kept at 0.6, 1.2, 1.8, 2.4 and 3.0 m/s because at higher sliding speeds the time of contact between the sliding surfaces decreases which in turn may leads to inaccurate results in terms of material removal in grams. However, the speed up to 8–10 m/s can be attained in the Ducom make pin-on-disc apparatus. The recommended sliding distance in wear tests is up to 4000 m, and keeping this in view, the authors have selected the levels of sliding distance as 400, 800, 1200, 1600 and 2000 m. The experimental plan for the wear tests is shown in Table 4 with coded and actual values of the four process parameters along with the results obtained in terms of weight loss.

3 Results and discussion

In situ TiB_2-reinforced composites were successfully fabricated via chemical reaction between K_2TiF_6 and KBF_4 using AA6082–T6 alloy. XRD patterns reveal the presence of TiB_2 particles in the matrix alloy and SEM micrographs show the even dispersion of reinforcements within the matrix.

The microhardness of the composites reinforced with 3, 6, 9 and 12 wt% of TiB_2 was improved by 2.97, 6.93, 12.88 and 15.84%, respectively, when compared to the unreinforced alloy. RSM analysis revealed that the wear in the composites decreases with the increase in reinforcement content and sliding speed whereas an increase in load or sliding speed or both results in enhancement of wear loss. Sliding distance was the most dominating variable to influence the wear behaviour of AA6082–T6/TiB_2 composites with a contribution of 65.28% followed by sliding speed (14.78%), load (9.39%) and reinforcement weight percentage (3.86%), respectively. The confirmation tests conducted to validate the present model showed that the difference between the experimental and the predicted results were below 6.5%, which is close enough to conclude that the present model is accurate and dry sliding wear behaviour of these composites were successfully evaluated using RSM.

3.1 Microstructure analysis

AA6082–T6/TiB_2 composites were fabricated by the in situ reaction of K_2TiF_6 and KBF_4 in the molten aluminium, and the XRD patterns of the composite reinforced with 3, 6, 9 and 12 wt% of TiB_2 are shown in Fig. 2. They all reveal the presence of TiB_2 in the composite. Trace amounts of titanium aluminide (Al_3Ti) and aluminium diboride (AlB_2) have been observed as they were the initial products of the exothermic reactions between K_2TiF_6 and KBF_4 [23]. The reaction between Ti and B produced TiB_2 and as the amount of TiB_2 increased, most Ti has been consumed and there was very limited amount of Ti for the formation of Al_3Ti particles. The reactions that take place are as follows [23]:

$$3Al + 2Ti + 2B \rightarrow TiB_2 + Al_3Ti$$
$$Ti + 2B \rightarrow TiB_2$$
$$Al + 2B \rightarrow AlB_2$$
$$Ti + 3Al \rightarrow Al_3Ti$$

SEM images of fabricated composites reinforced with 3, 6, 9, and 12 wt% of TiB_2 are given in Fig. 3a–d. They

Table 3 Factors and the levels used in CCD experimental plan

Factors	Designation	Levels				
		− 2	− 1	0	1	2
Reinforcement (wt%)	R	0	3	6	9	12
Sliding speed (m/s)	S	0.6	1.2	1.8	2.4	3.0
Load (N)	L	14.71	29.42	44.13	58.84	73.55
Sliding distance (m)	D	400	800	1200	1600	2000

Table 4 Details of test combinations in coded and actual values of factors and corresponding experimental results

Run no.	*R*	*S*	*L*	*D*	% Reinforcement, *R*	Speed, *S*	Load, *L*	Sliding distance, *D*	Wear Al–TiB_2 (g)
1	− 1	− 1	− 1	− 1	3	1.2	29.42	800	0.0072
2	1	− 1	− 1	− 1	9	1.2	29.42	800	0.0056
3	− 1	1	− 1	− 1	3	2.4	29.42	800	0.0033
4	1	1	− 1	− 1	9	2.4	29.42	800	0.0028
5	− 1	− 1	1	− 1	3	1.2	58.84	800	0.0099
6	1	− 1	1	− 1	9	1.2	58.84	800	0.0073
7	− 1	1	1	− 1	3	2.4	58.84	800	0.0066
8	1	1	1	− 1	9	2.4	58.84	800	0.0038
9	− 1	− 1	− 1	1	3	1.2	29.42	1600	0.0171
10	1	− 1	− 1	1	9	1.2	29.42	1600	0.0126
11	− 1	1	− 1	1	3	2.4	29.42	1600	0.0098
12	1	1	− 1	1	9	2.4	29.42	1600	0.0077
13	− 1	− 1	1	1	3	1.2	58.84	1600	0.0195
14	1	− 1	1	1	9	1.2	58.84	1600	0.0178
15	− 1	1	1	1	3	2.4	58.84	1600	0.0165
16	1	1	1	1	9	2.4	58.84	1600	0.0128
17	− 2	0	0	0	0	1.8	44.13	1200	0.0113
18	2	0	0	0	12	1.8	44.13	1200	0.0087
19	0	− 2	0	0	6	0.6	44.13	1200	0.0145
20	0	2	0	0	6	3	44.13	1200	0.0072
21	0	0	− 2	0	6	1.8	14.71	1200	0.0056
22	0	0	2	0	6	1.8	73.55	1200	0.0108
23	0	0	0	− 2	6	1.8	44.13	400	0.0015
24	0	0	0	2	6	1.8	44.13	2000	0.0186
25	0	0	0	0	6	1.8	44.13	1200	0.0090
26	0	0	0	0	6	1.8	44.13	1200	0.0086
27	0	0	0	0	6	1.8	44.13	1200	0.0079
28	0	0	0	0	6	1.8	44.13	1200	0.0087
29	0	0	0	0	6	1.8	44.13	1200	0.0073
30	0	0	0	0	6	1.8	44.13	1200	0.0082

depict that the dispersion of reinforcement was reasonably homogeneous within the matrix of AA6082 composites. However, as the amount of reinforcement increased in the composites, a small degree of agglomeration of TiB_2 particles has also been observed. Figure 3d which represents the SEM micrographs of 12 wt% of TiB_2-reinforced composites shows the clusters formation at some places due to the high percentage of TiB_2 particulates, but the performance of the composite has not deteriorated as evident from the Vickers tests which shows an increase in hardness and the wear tests which confirms the minimum material removal at 12 wt% of TiB_2. Moreover, it was also found from the literature that the agglomeration of particles can contribute towards strengthening of composite if well bonded in the matrix [24]. The size of the TiB_2 was also found to be larger in composites with higher TiB_2 content. The SEM images show no casting defects like porosity or shrinkage existed in the specimens. This indicates that the AA6082–T6/TiB_2 composites so produced were of good quality.

3.2 Microhardness analysis

Figure 4 shows the variation in microhardness of all the samples of AA6082–T6/TiB_2 composites. As was expected, the hardness of the in situ composites increased with the increase in wt% of TiB_2, which can be attributed to the inclusion of hard ceramic particles in the matrix which contributes towards resisting plastic deformation, thus leading to higher hardness. The more the addition of ceramic particles, the higher was the hardness [25]. The hardness of the composites reinforced with 3, 6, 9 and

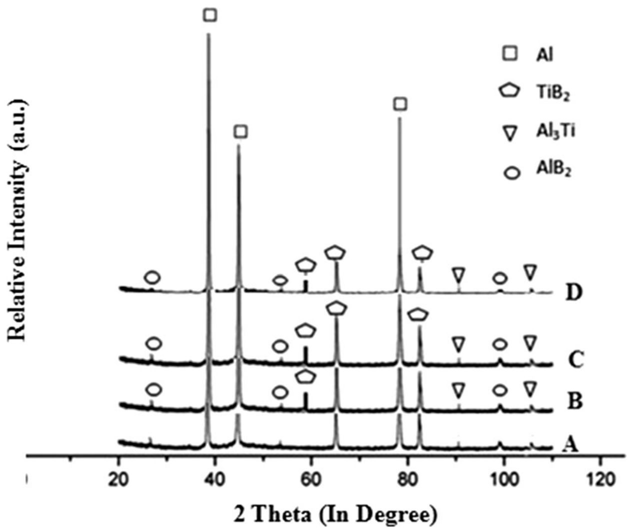

Fig. 2 XRD patterns for (A) 3 wt%, (B) 6 wt%, (C) 9 wt% and (D) 12 wt% of TiB_2-reinforced composites

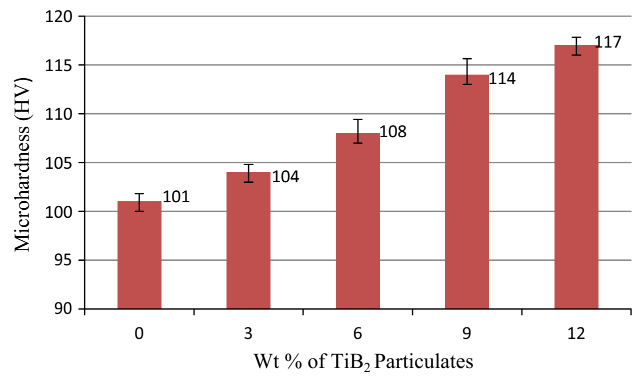

Fig. 4 Variation in microhardness of the AA6082–T6/TiB_2 composites with increase in reinforcement content

12 wt% of TiB_2 has been improved by 2.97, 6.93, 12.88, and 15.84%, respectively, when compared to the unreinforced alloy. Many other researchers reported the similar

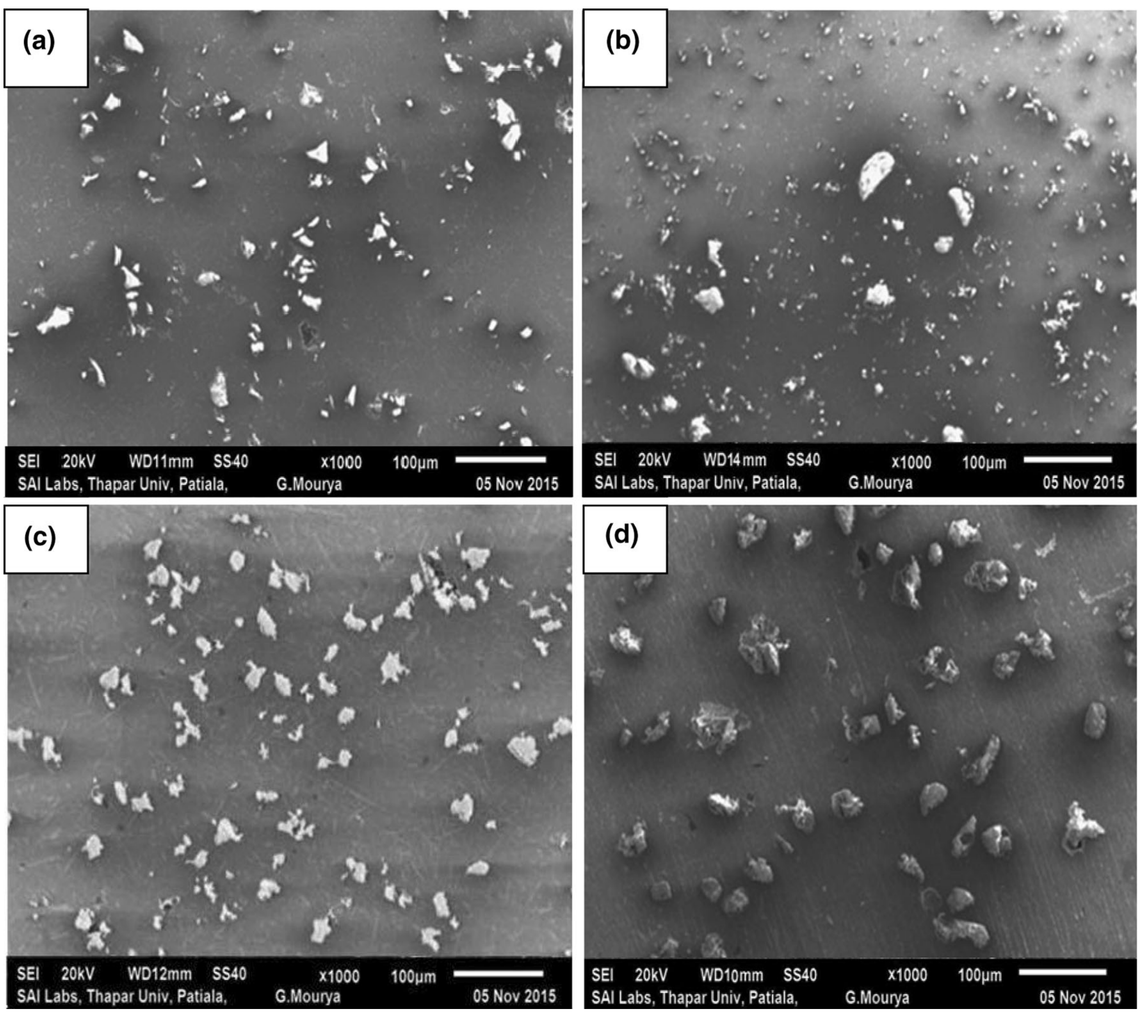

Fig. 3 SEM micrographs for **a** 3 wt%, **b** 6 wt%, **c** 9 wt% and **d** 12 wt% of TiB_2-reinforced composites

trend for the microhardness in the composites reinforced with TiB_2 particles [7, 26, 27]. In a study conducted by Rajan et al. [28], it was analysed that the improvement in hardness of TiB_2-reinforced composite was almost 50% as compared to the base material AA7075. However, the increase in hardness found in the composites studied in the present work seems to be relatively small and the one possible reason was the age-hardening, which made the alloy very hard already. As illustrated by the relatively small scattering in microhardness data for the composites with high TiB_2 contents, it also confirms that extent of clustering in these composites was not serious.

3.3 Analysis of variance (ANOVA) for wear behaviour

CCD was used in the present work to investigate the wear behaviour of Al6082–T6/TiB_2 composites. ANOVA was obtained using Design Expert 7.0.0 software to assess the significant factors and the interactions between the significant terms. ANOVA results for the present work are given in Table 5. The factors and their interactions have been categorized as significant or not significant, depending upon the confidence level or p value. In the present analysis, any factor or the interaction with a p value < 0.05 was considered as significant, as shown in Table 5. Only the significant factors were included in the wear model, while the non-significant factors were excluded using backward elimination. Lack of fit came out as not significant with p value 0.1793, much higher that the cut-off value of 0.05. All the four process parameters (reinforcement content, sliding speed, load and sliding distance) have been shown to be significant. The other significant factors apart from the four process parameters were the square terms of reinforcement, sliding speed and sliding distance as all have the p value < 0.05. The interaction between load and sliding distance ($L \times D$) was the only significant interaction in the present wear model. The percentage contribution of significant factors or their interaction can be calculated by Eq. (1).

$$\text{Percentage } (\%) \text{ contribution} = \frac{\text{Sum of squares of a factor}}{\text{Cor Total}} \times 100 \tag{1}$$

where Cor Total = totals corrected for the mean as noted from Table 5.

From the calculation, the influence of sliding distance was found to be the largest (% contribution = 65.28%), followed by sliding speed (14.78%), load (9.39%) and reinforcement content (3.86%). The reinforcement influence was the least among the four process parameters. This may be attributed to the limited hardness increment of the age-hardened composites owing to the reinforcements.

Table 5 ANOVA results for wear of AA6082–T6/TiB_2 composites

Source	Sum of squares	Degree of freedom	Mean square	F value	p value Prob > F	Percentage contribution	
Model	6.41×10^{-4}	8	8.01×10^{-5}	104.65	< 0.0001		Significant
Reinforcement (R)	2.54×10^{-5}	1	2.54×10^{-5}	33.17	< 0.0001	3.86	Significant
Sliding Speed (S)	9.72×10^{-5}	1	9.72×10^{-5}	126.86	< 0.0001	14.78	Significant
Load (L)	6.17×10^{-5}	1	6.17×10^{-5}	80.60	< 0.0001	9.39	Significant
Sliding Distance (D)	4.29×10^{-4}	1	4.29×10^{-4}	560.26	< 0.0001	65.28	Significant
LD	7.15×10^{-6}	1	7.15×10^{-6}	9.34	0.0060	1.08	Significant
R^2	6.10×10^{-6}	1	6.10×10^{-6}	7.97	0.0102	0.92	Significant
S^2	1.29×10^{-5}	1	1.29×10^{-5}	16.87	0.0005	1.96	Significant
D^2	6.43×10^{-6}	1	6.43×10^{-6}	8.40	0.0086	0.97	Significant
Residual	1.60×10^{-5}	21	7.66×10^{-7}			2.44	Significant
Lack of Fit	1.41×10^{-5}	16	8.86×10^{-7}	2.32	0.1793	2.15	Not significant
Pure Error	1.90×10^{-6}	5	3.81×10^{-7}			0.29	
Cor Total	6.57×10^{-4}	29					
SD	0.0008753		R^2		0.9755		
Mean	0.0096070		Adj R^2		0.9662		
C.V. %	9.11		Pred R^2		0.9470		
Press	0.0000348		Adeq precision		37.023		

Within this range of reinforcement contents, the maximum increase in hardness from unreinforced alloy to the composite with 12% TiB_2 was approximately ((117–101)/101) = 16%. This relatively small increment in hardness has limited effect on the wear resistance of the reinforcement, thus explaining the low percentage contribution of the reinforcement contents. The contributions of the interaction between load and sliding speed ($L \times D$) and the square terms was less than those owning to the four process parameters, as shown in Table 5. *F* value is the variance ratio, which is the ratio of variance due to factors effect and variance due to error term. The significance of the *F* value is that it helps in predicting the contribution of the factors used in the wear behaviour analysis. An increase in the *F* value of any factor signifies that the contribution of that factor is also increasing, which is also justified in the ANOVA results. The value of R^2 here shows the variability of the wear model to be 97.5%. The results shows that R^2 (0.9755) is greater than adjusted R^2 (0.9662), which is desirable for a good model as R^2 is influenced by both the significant and non-significant terms; whereas Adjusted R^2 includes significant terms only. Another significant sign in the present model is the difference between adjusted R^2 and predicted R^2 is less than 0.2, which confirms that the model adopted here was statistically satisfactory. The models adequacy can also be assured with their adequate precision, which must be greater than 4 for a fine model. In the present work, adequate precision value of 37.02 was obtained.

Equations (2) and (3) below represent the final equation in terms of coded factors and in terms of actual factors, respectively, which will be used further to explain the effect of the selected variables on wear (weight loss).

Equation for AA6082–T6/TiB_2 in terms of coded factors can be expressed as:

$$\begin{aligned}\text{Wear (g)} &= +8.306\times10^{-3} - 1.029\times10^{-3}\times R - 2.013\times10^{-3}\times S \\ &+ 1.604\times10^{-3}\times L + 4.229\times10^{-3}\times D + 6.688\times10^{-4}\times L\times D \\ &+ 4.670\times10^{-4}\times R^2 + 6.795\times10^{-4}\times B^2 + 4.79\times10^{-4}\times D^2\end{aligned} \tag{2}$$

Equation for AA6082–T6/TiB_2 in terms of actual factors can be expressed as:

$$\begin{aligned}\text{Wear (g)} &= +1.7219\times10^{-3} - 9.656\times10^{-3} \\ &\times R - 10.149\times10^{-3}\times S - 2.733\times10^{-5} \\ &\times L - 1.63467\times10^{-6}\times D + 1.136\times10^{-7} \\ &\times L\times D + 5.188\times10^{-5}\times R^2 \\ &+ 1.887\times10^{-3}\times S^2 + 2.996\times10^{-9}\times D^2\end{aligned} \tag{3}$$

The effects of individual factors are discussed by considering Eq. (2) because all the factors are at same level. The coefficient 8.306×10^{-3} in Eq. (2) represents the average wear in the composites [29]. The coefficient -1.029×10^{-3} associated with the amount of reinforcement has a negative value, which demonstrates a decline in wear with increasing TiB_2 content in the composites. As far as the sliding distance is concerned, Eq. (2) shows that the coefficient of $+4.229 \times 10^{-3}$ associated with sliding distance has a large positive value as compared to other coefficients. This signifies the sliding distance as the

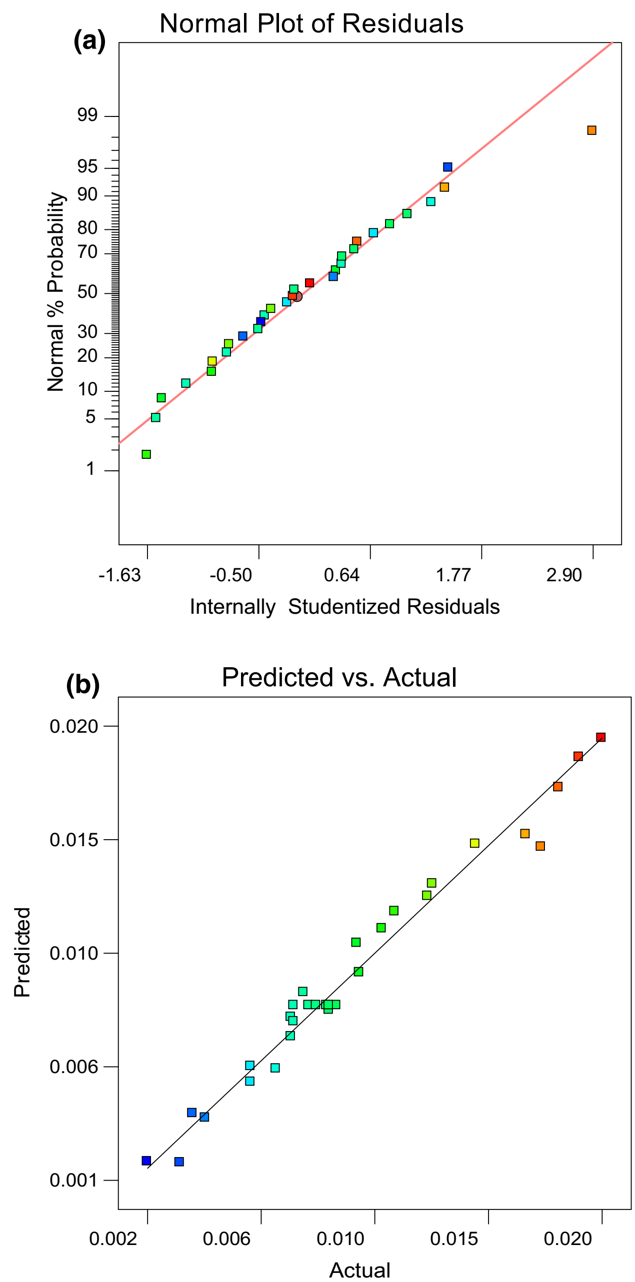

Fig. 5 **a** Normal plot of residuals and **b** predicted versus actual

predominant contributor in the wear of the composites studied; and the wear increased abruptly with the increase in the sliding distance.

Figure 5a shows a normal plot of residual for AA6082–T6/TiB_2 composites. The plot shows that most of the residuals are clustered along the inclined line, which verifies the normal distribution of ANOVA. Similar trend is followed by the residuals in the plot of predicted versus actual, as shown in Fig. 5b, which indicates a strong correlation between the model's prediction and its actual values.

3.4 Effect of variables on wear behaviour

As discussed above, the four process parameters have different levels of significance on the wear behaviour of AA6082–T6/TiB_2 composites studied. Figure 6a–d shows the effects of reinforcement content, sliding speed, load and sliding distance on the wear behaviour of the in situ composites. Similar to Eq. (2), Fig. 6a also reveals the similar trend, where it can be seen that the slope representing the amount of wear reduced with increasing amount of reinforcement. This decrease in wear was associated with the higher microhardness as the reinforcement content increased. An increase in hardness in the composites expectedly lowered the material removal rate in the composites, and thereby reduced the wear [30]. However, this trend was found to be relatively small when compared with those of other factors. The negative coefficient -2.013×10^{-3} associated with the sliding speed shows the similar trend of wear as observed with reinforcement. As the negative values are higher in case of sliding speed as compared to % reinforcement, this signifies that sliding speed has more detrimental effect than the

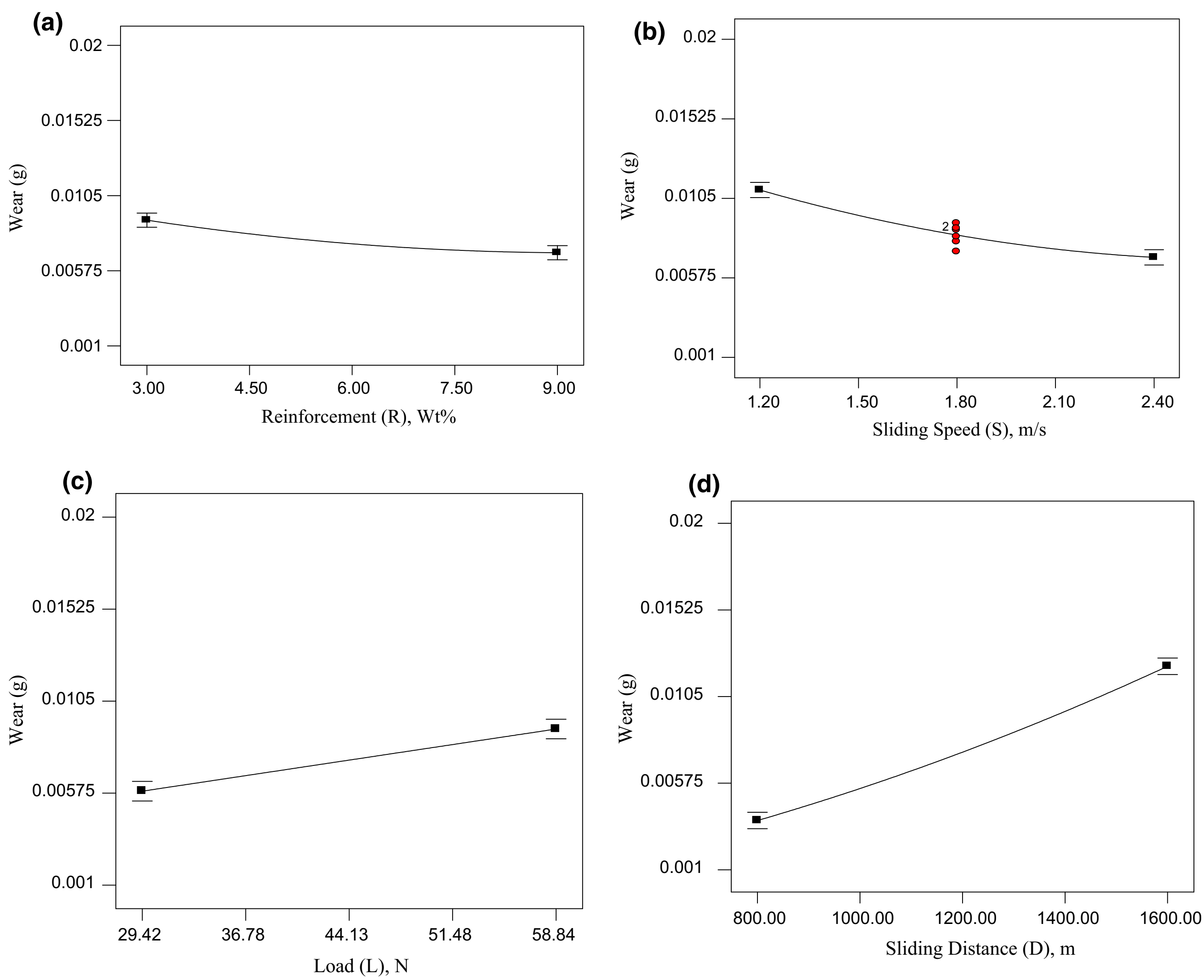

Fig. 6 Effect of individual factors on the dry sliding wear behaviour AA6082–T6/TiB_2 composites **a** Reinforcement (wt%); **b** sliding speed (m/s); **c** load (N) and **d** sliding distance (m)

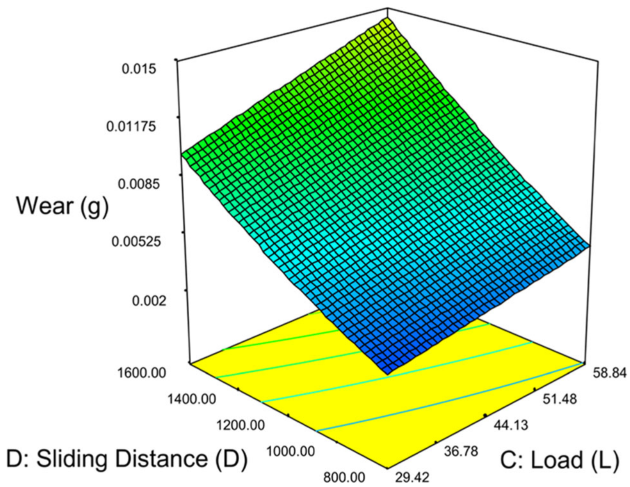

Fig. 7 3D interaction plot between load and sliding distance (LD) against the wear

reinforcement on the wear of AA6082–T6/TiB_2 composites. Increasing the sliding speed reduced the wear in TiB_2-reinforced composites, as also shown in Fig. 6b. The possible reason for this diminution in wear was the change in shear rate because of the increase in sliding speed, which perturbed the mechanical actions of the two surfaces in contact while sliding [31]. Higher sliding speed actually increased the strain rates in the material, which resulted in the reduction of the contact area and hence reduced the wear [32, 33]. Moreover, the positive coefficient $+\,1.604 \times 10^{-3}$ with load signifies that the wear was enhanced with the increase in load. The wear increases with increasing load because load determines the deformation and pressure applied in the two surfaces in contact. By increasing load, higher pressure is applied at the mating surfaces, which causes greater deformation and results in higher material removal. Figure 6c also shows the gradual increase in the wear with increasing load. Higher applied loads caused the plastic deformation of the contacts between the wear pin and the counter surface, and were accountable for a higher material removal. The graph of wear in Fig. 6d also reveals the importance of sliding distance. With an increase in the sliding distance, the interaction time between the wear pin and the counter surface increased; which finally resulted in an increase in wear.

ANOVA results shows that $L \times D$ was the only significant interaction in the present model. Figure 7 shows a 3D interaction plot of load and sliding distance, and it is evident that the sliding distance was the most dominating factor in increasing the wear, mainly due to the longer interaction time between the wear pin and the counter surface. Wear increased at both the lower (29.42 N) and higher (58.84 N) load with the escalation in sliding distance. The pressure which was created between the mating surfaces with the gradual increase in load caused deformation in the material and in turn high removal of material. Figure 7 shows that the minimum wear loss was attained at lower values of load and sliding distance and the combined effect of these two enhances wear in the composites.

3.5 Confirmation experiments

The final step in the dry sliding wear behaviour analysis of AA6082–T6/TiB_2 composites was to validate the developed model. Confirmation tests were carried out using three different sets of the four process parameters (reinforcement content, sliding speed, load, and sliding distance) as shown in Table 6. SEM micrographs of the specimens that were used in the confirmation tests are shown in Fig. 8a–c. The pitting on the surface of the alloy in Fig. 8b is due to the passive nature of the aluminium metal which when exposed to the atmosphere at room temperature, tends to form an oxide layer on the surface [34]. During the rubbing of the composite surface against the EN31 steel disc, the reinforced debris in the composite material might get detected from the oxide layer which results in small Pitts. The hardness tests and the adequate wear model that was developed in the present study shows that these smaller Pitts do not have any adverse effect on the study of wear behaviour analysis of the composites. One thing that was common among all the SEM micrographs was the presence of wide parallel lines in the sliding direction which eventually gets crushed off in the form of debris. The results obtained in the three experiments were recorded in the form of weight loss in grams and compared with the results attained through the quadratic model (Table 7). It was evident from Table 7 that the difference between the experimental and the predicted results were below 6.5%, which are small enough to conclude that the

Table 6 Set of parameters used in the confirmation tests

Test no.	Reinforcement (wt%)	Sliding speed (m/s)	Load (N)	Sliding distance (m)
1	9	2.4	29.42	800
2	6.4	2.4	29.42	800
3	5.5	2.3	50.20	800

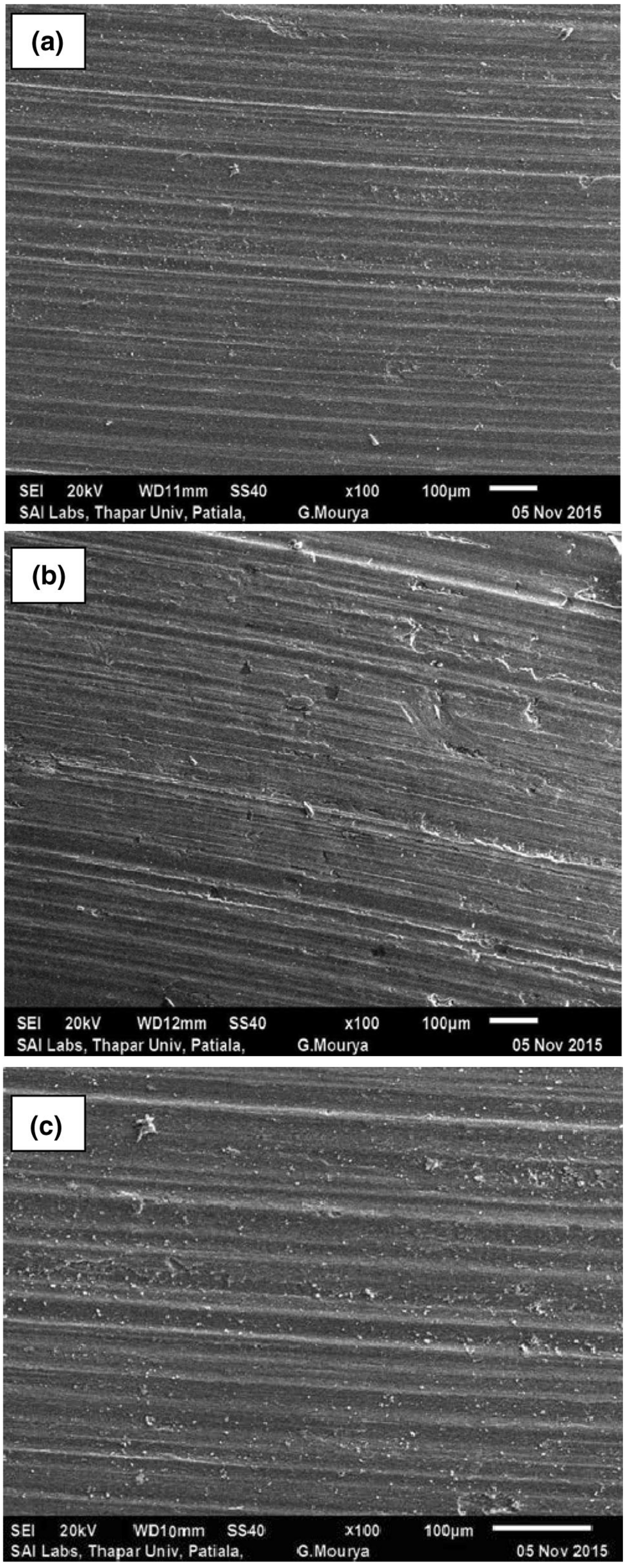

Fig. 8 SEM micrographs showing worn surfaces of AA6082–T6/TiB_2 composites used for confirmation tests **a** Test 1, **b** Test 2 and **c** Test 3

Table 7 Experimental and modelled results with error

Test no.	Experimental results	Modelled results	% Error
1	0.00180	0.00175	3.31
2	0.00224	0.00215	4.01
3	0.00485	0.00454	6.39

present model and the wear analysis are appropriate and can be used as predictive tools for wear applications.

4 Conclusions

This work demonstrates the feasibility of using response surface methodology to predict accurately the dry sliding wear behaviour of TiB_2-reinforced AMCs fabricated by stir casting. Following conclusions can be drawn from the present work:

1. In situ TiB_2-reinforced composites were successfully fabricated via chemical reaction between K_2TiF_6 and KBF_4 using AA6082–T6 alloy. The TiB_2 particles were found to be distributed in the matrix alloy relatively uniformly, although a small degree of clustering was found with increasing amount of TiB_2.
2. The microhardness of the composites reinforced with 3, 6, 9 and 12 wt% of TiB_2 was improved by 2.97, 6.93, 12.88, and 15.84%, respectively, when compared to the unreinforced alloy
3. RSM analysis revealed that the wear in the composites decreases with the increase in reinforcement content and sliding speed whereas an increase in load or sliding speed or both results in significant wear loss.
4. Sliding distance was the most dominating variable to influence the wear behaviour of AA6082–T6/TiB_2 composites with a contribution of 65.28% followed by sliding speed (14.78%), load (9.39%), and reinforcement weight percentage (3.86%), respectively.
5. The confirmation tests conducted has validated the present model, with the difference between the experimental and the predicted results below 6.5%. This is close enough to conclude that the present model is accurate.
6. The model developed with RSM results in good prediction of the wear of hybrid composite within the range of applied factors. The errors between the modelled and experimental results are within 3–7%, thus validating the developed wear predictive models.

Acknowledgements The authors wish to express their gratitude to the authorities of Mechanical Engineering Department, Thapar

University, Patiala, for providing the experimental facilities to conduct the work for this study.

References

1. Dwivedi SP, Sharma S, Mishra RM (2015) Microstructure and mechanical behavior of A356/SiC/Fly-ash hybrid composites produced by electromagnetic stir casting. J Braz Soc Mech Sci Eng 37:57–67
2. Sahin Y, Ozdin K (2008) A model for the abrasive wear behaviour of aluminium based composites. Mater Des 29:728–733
3. Tee KL, Lu L, Lai MO (1999) Synthesis of in situ Al–TiB_2 composites using stir cast route. Compos Struct 47:589–593
4. Natrajan S, Narayanasamy R, Kumaresh SP, Dinesh G, Anil B, Sivaprasad K (2009) Sliding wear behaviour of Al 6063/TiB_2 in situ composites at elevated temperatures. Mater Des 30:2521–2531
5. Suresh S, Shenbag N, Moorthi V (2012) Aluminum–titanium diboride (Al–TiB_2) metal matrix composites: challenges and opportunities. Proc Eng 38:89–97
6. Mandal A, Chakraborty M, Murty BS (2007) Effect of TiB_2 particles on sliding wear behaviour of Al–4Cu alloy. Wear 262:160–166
7. Kumar S, Chakraborty M, Subramanya SV, Murthy BS (2008) Tensile and wear behaviour of in situ Al–7Si/TiB_2 particulate composites. Wear 265:134–142
8. Mandal A, Murty BS, Chakraborty M (2009) Sliding wear behaviour of T6 treated A356–TiB_2 in situ composites. Wear 266:865–872
9. Mallikarjuna C, Shashidhara SM, Mallik US, Parashivamurthy KI (2011) Grain refinement and wear properties evaluation of aluminum alloy 2014 matrix-TiB_2 in situ composites. Mater Des 32:3554–3559
10. Ramesh CS, Ahamed A (2011) Friction and wear behaviour of cast Al 6063 based in situ metal matrix composites. Wear 271:1928–1939
11. Niranjan K, Lakshminarayanan PR (2013) Dry sliding wear behaviour of in situ Al–TiB_2 composites. Mater Des 47:167–173
12. Radhika N, Raghu R (2015) Dry sliding wear behaviour of aluminium Al–Si12Cu/TiB_2 metal matrix composite using response surface methodology. Tribol Lett 59:1–9
13. Lee HL, Lu WH, Chan SLI (1992) Abrasive wear of powder metallurgy Al alloy 6061–SiC particle composites. Wear 159:223–231
14. Lee HL, Lu WH, Chan SLI (1995) Effect of aging on the sliding abrasive wear of P/M 2014 and 6061 Al alloy–SiC particle composites. Mater Lett 15:49–52
15. Kang YC, Chan SLI (2004) Tensile properties of nanometric Al_2O_3 particulate-reinforced aluminum matrix composites. Mater Chem Phys 85:438–443
16. Lee IS, Hsu CJ, Chen CF, Ho NJ, Kao PW (2011) Particle-reinforced aluminum matrix composites produced from powder mixtures via friction stir processing. Compos Sci Technol 71:693–698
17. Ceschini L, Minak G, Morri A (2006) Tensile and fatigue properties of the AA6061/20 vol% Al_2O_{3p} and AA7005/10 vol% Al_2O_{3p} composites. Compos Sci Technol 66:333–342
18. Arasu PT, Dhanasekaran R, Kumar PS, Srinivasan N (2013) Effect of hardness and microstructure on En 353 steel by heat treatment. Int J Eng Sci 2:1–5
19. Rabinowicz ED (1965) Friction and wear of work hardening in the design of wear resistant materials. Wiley, New York, pp 168–174
20. Kumar R, Dhiman S (2013) A study of sliding wear behaviors of Al-7075 alloy and Al-7075 hybrid composite by response surface methodology analysis. Mater Des 50:351–359
21. Baradeswaran A, Vettivel SC, Perumal AE, Selvakumar N, Franklin Issac R (2014) Experimental investigation on mechanical behaviour, modelling and optimization of wear parameters of B4C and graphite reinforced aluminium hybrid composites. Mater Des 63:620–632
22. Montgomery DC (2007) Design and analysis of experiments. Wiley India (P) Ltd, New Delhi
23. Yue NL, Lu L, Lai MO (1999) Application of thermodynamic calculation in the in situ process of Al/TiB_2. Compos Struct 47:691–694
24. Ma ZY, Tjong SC, Li YL, Liang Y (1997) High temperature creep behavior of nanometric Si_3N_4 particulate reinforced aluminium composite. Mater Sci Eng, A 225:125–134
25. Singh G, Goyal S (2016) Dry sliding wear behaviour of AA6082–T6/SiC/B4C hybrid metal matrix composites using response surface methodology. Proc Inst Mech Eng L J Mater Des Appl. https://doi.org/10.1177/1464420716657114
26. Ramesh CS, Pramod S, Keshavamurthy R (2011) A study on microstructure and mechanical properties of Al 6061–TiB_2 in situ composites. Mater Sci Eng, A 528:4125–4132
27. Mandal A, Murty BS, Chakraborty M (2009) Wear behaviour of near eutectic Al–Si alloy reinforced with in situ TiB_2 particles. Mater Sci Eng, A 506:27–33
28. Michael Rajan HB, Ramabalan S, Dinaharan I, Vijay SJ (2013) Synthesis and characterization of in situ formed titanium diboride particulate reinforced AA7075 aluminum alloy cast composites. Mater Des 44:438–445
29. Sharma P, Sharma S, Khanduja D (2015) Parametric study of dry sliding wear behaviour of hybrid metal matrix composite produced by a novel process. Metall Mater Trans A 46A:3260–3270
30. Sharma N, Khanna R, Singh G, Kumar V (2016) Fabrication of 6061 aluminium alloy reinforced with Si_3N_4/n-Gr and its wear performance optimization using integrated RSM-GA. Part Sci Technol. https://doi.org/10.1080/02726351.2016.1196276
31. Chowdhury MA, Khalil MK, Nuruzzaman DM (2011) Effect of sliding speed and normal load on friction and wear property of aluminum. Int J Mech Mechatron Eng 11:45–49
32. Bhushan B, Jahsman WE (1978) Propagation of weak waves in elastic–plastic and elastic–viscoplastic solids with interfaces. Int J Solids Struct 14:39–51
33. Bhushan B, Jahsman WE (1978) Measurement of dynamic material behaviour under nearly uniaxial strain condition. Int J Solids Struct 14:739–753
34. Szklarska-Smialowska Z (1998) Pitting corrosion of aluminum. Corros Sci 41:1743–1767